

MBS: Macroblock Scaling for CNN Model Reduction

Yu-Hsun Lin

HTC Research & Healthcare
lyman.lin@htc.com

Chun-Nan Chou

HTC Research & Healthcare
jason.cn.chou@htc.com

Edward Y. Chang

HTC Research & Healthcare
edward.chang@htc.com

Abstract

We estimate the proper channel (width) scaling of Convolution Neural Networks (CNNs) for model reduction. Unlike the traditional scaling method that reduces every CNN channel width by the same scaling factor, we address each CNN macroblock adaptively depending on its information redundancy measured by our proposed *effective flops*. Our proposed macroblock scaling (MBS) algorithm can be applied to various CNN architectures to reduce their model size. These applicable models range from compact CNN models such as MobileNet (25.53% reduction, ImageNet) and ShuffleNet (20.74% reduction, ImageNet) to ultra-deep ones such as ResNet-101 (51.67% reduction, ImageNet) and ResNet-1202 (72.71% reduction, CIFAR-10) with negligible accuracy degradation. MBS also performs better reduction at a much lower cost than does the state-of-the-art optimization-based method. MBS’s simplicity and efficiency, its flexibility to work with any CNN model, and its scalability to work with models of any depth makes it an attractive choice for CNN model size reduction.

Introduction

CNN models have been widely used by image-based applications, thanks to the breakthrough performance of AlexNet (Krizhevsky, Sutskever, and Hinton 2012) and VGGNet (Simonyan and Zisserman 2014). However, a very deep and wide CNN model consists of many parameters, and as a result, the trained model may demand a large amount of DRAM and a large number of multiplications to perform a prediction. Such high resource and computation requirements lead to latency, heat, and power consumption problems, which are suboptimal for edge devices such as mobile phones and IoTs (Sze et al. 2017). Therefore, reducing CNN model size is essential for improving resource utilization and conserving energy.

Several CNN model reduction algorithms have recently been proposed (Sze et al. 2017). These algorithms can be divided into two categories: micro-level (e.g., performing reduction/quantization inside a filter) and macro-level reduction (e.g., removing redundant filters). These two categories are complements of each other. (More details are presented in the related work section.)

There are two macro-level reduction approaches: *optimization based* and *channel-scaling based*. Each approach has multiple methods and algorithms. The optimization-based approach typically estimates the filter importance by formulating an optimization problem with the adopted criteria (e.g., filter weight magnitude). Removing a filter (or a channel) will affect both the former and latter layers. The filter pruning step of the optimization-based method must take into account the inter-connected structures between CNN layers. Therefore, a CNN model such as DenseNet (Huang et al. 2017) and ShuffleNet (Zhang et al. 2017) with more complex inter-connected structures may prevent the optimization-based approach from being effective.

The channel-scaling based approach using an α -scaler to reduce channel width. For instance, MobileNet (Howard et al. 2017) uses the same α -scaler to prune the widths of all channels. Applying the same α -scaler to all convolutional layers without considering each information density is a coarse-grained method. A fine-grained method that finds the optimal α -scaler for each convolutional layer should be ideal. However, the increasingly complicated inter-layer connection structures of CNN models forbid fine-grained scaling to be feasible. In addition, a layer-dependent method requires a dependable metric to measure information redundancy for each convolution layer to determine an effective layer-dependent scalar.

To address the shortcomings of the current model-compaction methods, we propose *macroblock scaling* (MBS). A macroblock consists of a number of convolution layers that exhibit similar characteristics, such as having the same resolution or being a segment of convolution layers with customized inter-connects. Having macroblock as a structure abstraction provides the flexibility for MBS to inter-operate with virtually any CNN models of various structures, and also permits channel-scaling to be performed in a “finer”-grained manner. To quantify information density for each macroblock so as to determine an effective macroblock-dependent scalar, MBS uses *effective flops* to measure each macroblock’s information density. (We define *effective flops* to be the number of convolution flops required for the activated non-zero ReLU outputs.) Experimental results show that the reduction MBS can achieve is more significant than those achieved by all prior schemes.

In summary, the contributions of this work are as follows:

Table 1: Comparison between the optimization-based and the scaling-based approaches for model reduction.

Property	Optimization-based	Scaling-based
Performance	High	Medium-High
Flexibility	Low	High
Scalability	Low	High

- MBS employs *macroblock* to address the issues that both coarse-grained and fine-grained scaling cannot deal with, and hence allows channel-scaling to be performed with any CNN models.
- MBS proposes using an effective and efficient measure, *effective flops*, to quantify information density to decide macroblock-dependent scaling factors. As shown in the algorithm section, the computation complexity of MBS is linear w.r.t. the number of training instances times the number of parameters, which is more efficient than the optimization-based methods.
- Extensive empirical studies on two representative datasets and all well-known CNN models (e.g., MobileNet, ShuffleNet, ResNet, and DenseNet) demonstrate that MBS outperforms all state-of-the-art model-reduction methods in reduction size while preserving the same level of prediction accuracy. Due to its simple and effective nature, MBS remains to be effective even with ultra-deep CNNs like ResNet-101 on ImageNet (51.67% reduction) and ResNet-1202 on CIFAR-10 (72.71% reduction).

The remaining parts of this paper are organized into three main sections. The Related Work section highlights some previous efforts of reducing CNN models. The Method section explains our proposed MBS algorithm. The Experiment section shows the encouraging results of applying MBS on various CNN models.

Related Work

We review related work in two parts. We first review key CNN properties relevant to the inception of MBS and then review some representative model-reduction methods.

Relevant CNN Properties

There are research works (Teerapittayanon, McDanel, and Kung 2016; Figurnov et al. 2017; Wu et al. 2018) integrating the early stop (or early exit) mechanism of the initial CNN layers in order to speed up the inference process. This phenomenon demonstrates that the outcome of a CNN model at early stages can be adequate for predicting an image label with high confidence. This result provides supporting evidence for us to group convolution layers into two types: former convolution layers (near to the input image) as the base layers, and latter convolution layers (close to the label output) as the enhancement layers. The early stop mechanism motivates that the information density in the enhancement

layers should be lower than that in the base layers, and therefore, more opportunities exist in the enhancement layers to be compressed to reduce model size.

Reduction Methods of CNN Model

As mentioned in the introduction that model reduction can be divided into micro-level and macro-level approaches. Binary approximation of a CNN filter is one important direction for micro-level model reduction (Courbariaux, Bengio, and David 2015; Rastegari et al. 2016; Lin, Zhao, and Pan 2017; Hubara et al. 2016; Rastegari et al. 2016). Maintaining prediction accuracy of a binary CNN is a challenging issue (Tang, Hua, and Wang 2017). The sparse convolution modules (Liu et al. 2015; Wen et al. 2016; Jaderberg, Vedaldi, and Zisserman 2014; Denton et al. 2014; Aghasi et al. 2017) or deep compression (Han, Mao, and Dally 2016) usually introduce irregular structures. However, these micro-level model reduction methods with irregular structures often require special hardware for acceleration (Han et al. 2016).

The macro-level model reduction approach removes irrelevant filters and maintains the existing structures of CNNs (Li et al. 2017; He, Zhang, and Sun 2017; Liu et al. 2017; Hassibi and Stork 1993). The methods of this reduction approach estimate the filter importance by formulating an optimization problem based on some adopted criteria (e.g., the filter weight magnitudes or the filter responses). The research work of (Yu et al. 2018) addresses the filter importance issue by formulating the problem into binary integer programming with the aid of feature ranking (Roffo, Melzi, and Cristani 2015), which achieves the state-of-the-art result. For an n -layers model with n_p parameters and N training images, the computational complexity of the feature ranking preprocessing is $O(n_p \times N)$ to acquire the corresponding CNN outputs of the N training images, and the ranking step would take additional $O(N^{2.37})$ complexity (Roffo, Melzi, and Cristani 2015). In addition to the pre-processing step, the binary integer programming is an NP-hard problem. The detail complexity is not specified in (Yu et al. 2018). In general, a good approximate solution for n_p variables still requires high computational complexity (e.g., $O(n_p^{3.5})$ by linear programming (Karmarkar 1984)).

MBS enjoys low computation complexity that is $O(n_p \times N)$ in computing information density and $O(n_p)$ in computing the scaling factors (Algorithm 1 in the next section presents details). MBS enjoys superior model-reduction ratio while preserving prediction accuracy at low computation cost.

MBS Algorithm

This section presents our proposed macroblock scaling (MBS) algorithm for reducing an already trained CNN model. We first define key terms including *channel*, *filter*, *channel scaling*, *macroblock*, and parameters used by MBS. We then explain how MBS computes information density, and how that information is used by MBS to reduce model size. Finally, we analyze computational complexity

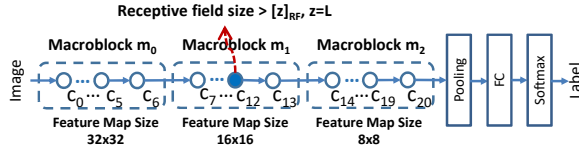


Figure 1: An example CNN model for the CIFAR image (32×32 pixels) that contains three CNN macroblocks. Each macroblock m_i consists of the CNN layers with the same output size of feature map (i.e., same width and height).

of MBS and compare its efficiency with competing model-compaction algorithms.

We use image applications to explain a CNN pipeline. A typical CNN pipeline accepts N training images as input. These N training instances are of the same height and width. To simplify our notation, we assume all input images are in the square form with the same resolution $L \times L$. A CNN model is composed of multiple convolution layers. The input to a convolution layer is a set of input tensors (or input activations), each of which is called a *channel* (Sze et al. 2017). Each layer generates a successively high-level abstraction of the input tensors, call a output tensor or feature map.

More specifically, the j^{th} convolution layer c_j , $j = 0, \dots, n-1$, takes $D_u \times D_u \times w_{j-1}$ input tensor u and produces $D_v \times D_v \times w_j$ output tensor v , where D_u is the spatial height and width of u , w_{j-1} the input channel width (i.e., number of channels), D_v the spatial height and width of v , and w_j the output channel width. Let D_k denote the spatial dimension of the square-filter kernel of c_j , the required number of parameters of c_j can be written as

$$D_k \times D_k \times w_{j-1} \times w_j. \quad (1)$$

MBS groups convolution layers into *macroblocks*. Macroblock consists of the convolution layers whose output tensors (feature maps) are of the same size. Figure 1 depicts an example CNN model with three CNN macroblocks. The size of output tensors is down-sampled by the pooling layers with stride size 2. Hence, macroblock m_i is defined as

$$m_i = \{c_j \mid D_v = \frac{L}{2^i}\}. \quad (2)$$

Operation *scaling* reduces channel width. Intuitively, MBS would like to prune channels that cannot provide positive contributions to accurate prediction. For instance, MobileNet (Howard et al. 2017) scales down all channel widths by a constant ratio $0 < \alpha < 1$, or we call this baseline scheme α -scaling. MobileNet uses the same α value for all convolution layers. However, an effective channel-scaling scheme should estimate the best scaling ratio for each convolutional layer based on its *information density*, which MBS quantifies and determines layer-dependent α values.

Grouping Layers on Information Density

An effective CNN model requires a sufficient number of convolution layers to capture good representations from input data. However, as the number of the convolution lay-

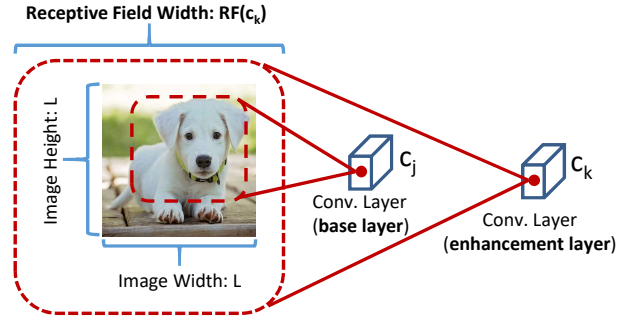


Figure 2: An example of the receptive field of the neuron in the CNN base layer c_j and the CNN enhancement layer c_k .

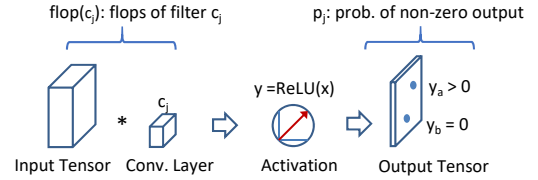


Figure 3: Effective flop calculates of the flops considering the non-zero probability p_j of the ReLU output.

ers grows beyond a threshold, the additional benefit in improving prediction accuracy can diminish. One may argue that the former convolution layers may learn low-level representations such as edges and contours, whereas latter layers high-level semantics. As we will demonstrate shortly, the latter layers may cover *receptive fields* that are larger than the input images, and their learned information may not contribute to class prediction. The effective receptive field in CNN is the region of the input image that affects a particular neuron of the network (Luo et al. 2016). Figure 2 shows an example, where a neuron of a former convolution layer covers a region inside the input image, whereas a neuron of a latter layer may cover a region larger than the input image.

Hence, we categorize convolution layers into two types, base layers and enhancement layers, which are defined as follows:

- **Base convolution layers:** The former convolution layers (near to the input) of a CNN model learn essential representations from the training data. Though representations captured in the base layers could be redundant, they are fundamental for accurate class prediction.
- **Enhancement convolution layers:** The latter convolution layers may cover receptive fields larger than the input areas¹. Therefore, opportunities are available for channel pruning to remove both useless and redundant information.

¹Due to data augmentation and boundary patching operations applied to raw input images, a training input image may contain substantial useless information at its boundaries.

Determining CNN Base Layers by Receptive Field

Revisit macroblocks in Figure 1. Convolution layer c_{12} belonging to macroblock m_1 is the first enhancement layer, where its receptive field is larger than the size of the input image. We estimate information redundancy of each macroblock m_i by measuring the information density ratio contributed by the enhancement layers.

Now, we define a function $\text{RF}(c_j)$ to compute the receptive field size of layer c_j . For simplicity, assume that the receptive field region of filter c_j is $\text{RF}(c_j) \times \text{RF}(c_j)$. The possible set of values of $\text{RF}(c_j)$ is discrete, which is determined by the configuration of the kernel size and the stride step of a CNN model. For lucid exposition, we define $\lceil z \rceil_{\text{RF}}$ to characterize the minimum receptive field boundary that is greater than a given value z as follows:

$$\lceil z \rceil_{\text{RF}} = \min\{\text{RF}(c_j) \mid \text{RF}(c_j) > z \forall j\}. \quad (3)$$

We use this boundary $\lceil z \rceil_{\text{RF}}$ to divide base convolution layers and enhancement convolution layers in a CNN pipeline.

We can determine the base layers of a CNN by setting the value of z . As we have previously explained, the area beyond and at the boundary of an image contains less useful information. Therefore, setting $z = L$ is reasonable to separate those layers that can contribute more to class prediction from the other layers. A macroblock can contain base convolution layers only, enhancement layers only, or a mixture of the two.

Macroblock-level Reduction

To preserve the design structure of an original CNN model, MBS performs reduction at the macroblock level instead of at the convolution-layer level. As we defined in the beginning of this section, each macroblock contains convolutions layers of the same resolution. In addition, for some CNN models that have convolution layers connected into a complex structure, MBS treats an entire such segment as a macroblock to preserve its design. Our macroblock approach, as its name suggests, does not deal with detailed inter-layer connection structure. The macroblock abstraction thus makes model reduction simple and adaptive.

Macroblock Information Density/Redundancy Estimation

MBS uses *convolution FLOP* to estimate information density. A FLOP (denoted by the lowercase ‘‘flop’’ in the remainder of the paper) is a multiply-and-add operation in convolution. The more frequently that ReLU outputs a zero value means that the less information that convolution layer contains. Therefore, only those flops that can produce a non-zero ReLU output is considered to be effective. Figure 3 shows the computation of the effective flops of a convolution layer. Let e_{c_j} denote effective flops of layer c_j , and p_j the non-zero probability of its ReLU output. We can define e_{c_j} as

$$e_{c_j} = p_j \times \text{flop}(c_j). \quad (4)$$

To evaluate information density of macroblock m_i , we tally the total effective flops from the beginning of the CNN

pipeline to the end of macroblock m_i . We can write the sum of the effective flops as

$$E_{\text{total}}(m_i) = \sum e_{c_j}, c_j \in \{m_0, \dots, m_i\}. \quad (5)$$

Next, we compute the effective flops in the base layers or those flops taking place within the receptive field as

$$E_{\text{base}}(m_i) = \sum e_{c_j}, c_j \in \{\text{RF}(c_j) \leq \lceil z \rceil_{\text{RF}}\} \quad (6)$$

where the base layers have the maximum receptive field size $\lceil z \rceil_{\text{RF}}$.

Based on the total flops $E_{\text{total}}(m_i)$ and base flops $E_{\text{base}}(m_i)$, we define the difference between the two as the enhancement flops, which is denoted as $E_{\text{enhancement}}(m_i)$ and can be written as $E_{\text{total}}(m_i) - E_{\text{base}}(m_i)$. The redundancy ratio r_i of macroblock m_i is then defined as the total enhancement flops over the total flops, or

$$r_i = \frac{E_{\text{enhancement}}(m_i)}{E_{\text{total}}(m_i)} = 1 - \frac{E_{\text{base}}(m_i)}{E_{\text{total}}(m_i)}. \quad (7)$$

We estimate the channel-scaling factor for each macroblock m_i based on this derived redundancy r_i , which is addressed next.

Channel-Scaling Factor Estimation

We define the relation between the original channel width w_{m_i} of macroblock m_i and the compact channel width $w_{m_i}^c$ after the reduction process, which is depicted as

$$w_{m_i} = (1 + r_i)w_{m_i}^c. \quad (8)$$

If there is no redundancy in macroblock m_i (i.e., $r_i = 0$), the original channel w_{m_i} is equal to the compact channel width $w_{m_i}^c$. Therefore, the channel width multiplier β_i for the macroblock m_i is

$$\beta_i = \frac{1}{1 + r_i}, \quad (9)$$

where this estimation makes $\beta_i > 0.5$ since $r_i < 1$ according to Eq. (7). The lower bound of the channel-scaling factor β_i is in accordance with the observation made by MobileNet (Howard et al. 2017) that a scaling factor that is less than 0.5 can introduce noticeable distortion.

Algorithm 1 presents our MBS algorithm, which estimates the scaling factor β_i for each macroblock m_i and derives the compact channel width $w_{m_i}^c$. The MBS scaling algorithm takes the pre-trained model $F_n()$ with n convolution layers and the N training images as input. The convolution results of the pre-trained model $F_n()$ for the training images are utilized for estimating the scaling factors. The inner loop from steps 2 to 4 collects non-zero statistics of the ReLU outputs p_j . The steps in the outer loop after the inner loop (steps 5 and 6) take an average over N training instances, and then derive the effective flop for each convolution layer c_j .

The macroblock process starts from step 8. The MBS algorithm first tallies the total flops for each macroblock (steps 9 to 11). MBS then computes the base flops and redundant ratio r_i for macroblock m_i (steps 12 to 20). The scaling factor β_i is derived from redundancy ratio r_i in step 17. After

Algorithm 1 Macroblock Scaling

Input: $F_n()$, $I_{0 \sim N-1}$ /* Pre-trained Model, training images**Output:** $[w_{m_0}^c, w_{m_1}^c, \dots, w_{m_{k-1}}^c]$ /* Compact channel**Procedure:**

- $\text{NZ}()$ /* Computes the number of non-zero elements
- $\text{RF}()$ /* Computes receptive field size
- $\text{flop}()$ /* Computes the number of FLOPs

Variable:

- v_j^I /* The j^{th} ReLU output tensor of $F_n(I)$

BEGIN

```
1: for  $j = 1, \dots, n$  do
2:   for  $i = 0, \dots, N - 1$  do
3:      $p_j^{I_i} \leftarrow \frac{\text{NZ}(v_j^{I_i})}{D_{v_j} \times D_{v_j} \times w_j}$ 
4:   end for
5:    $p_j \leftarrow \frac{1}{N} \sum p_j^{I_i}$ 
6:    $e_{c_j} \leftarrow p_j \times \text{flop}(c_j)$ 
7: end for
8: for  $i = 0, \dots, k - 1$  do
9:   if  $c_j \in \{m_0, \dots, m_i\}$  then
10:     $E_{\text{total}}(m_i) \leftarrow \sum e_{c_j}$ 
11:   end if
12:   if  $c_j \in \{\text{RF}(c_j) \leq \lceil z \rceil_{\text{RF}}\}$  then
13:     $E_{\text{base}}(m_i) \leftarrow \sum e_{c_j}$ 
14:   end if
15:   if  $E_{\text{total}}(m_i) > E_{\text{base}}(m_i)$  then
16:     $r_i \leftarrow 1 - \frac{E_{\text{base}}(m_i)}{E_{\text{total}}(m_i)}$ 
17:     $\beta_i \leftarrow \frac{1}{1+r_i}$ 
18:   else
19:     $\beta_i \leftarrow 1$ 
20:   end if
21:    $w_{m_i}^c \leftarrow \lceil \beta_i \times w_{m_i} \rceil$  /* Estimate compact channel
22: end for
23: return  $[w_{m_0}^c, w_{m_1}^c, \dots, w_{m_{k-1}}^c]$ 
```

END

β_i has been computed, MBS estimates the compact channel width $w_{m_i}^c$ for each macroblock m_i in step 21.

After algorithm 1 outputs the new set of channel widths, the CNN is retrained with this set of new parameters to generate a more compact model $F'_n()$. In the experimental section, we will evaluate the effectiveness of MBS by examining the performance (prediction accuracy and model-size reduction) achieved by $F'_n()$ over $F_n()$.

The pre-trained model $F_n()$ has n_p parameters and N training images. The required complexity of MBS consists of two parts: the non-zero statistics p_j collection (from steps 1 to 7) and the redundancy r_i estimation (from steps 8 to 23). In the first part, we collect p_j by inferring the N training images, which the statement in step 3 can be absorbed into the forward pass of the pre-trained model. Hence, the computational complexity is $O(n_p \times N)$. The second part traverses all the convolution layers of the pre-trained model for computing the effective flops. The complexity of the second part is $O(n_p)$ in the pre-trained model $F_n()$. The wall-clock time of first part usually takes

Table 2: Model reduction results of ResNet on CIFAR-10.

Model	Acc. [Diff.]	Saving
ResNet-20	91.86%	-
MBS (L)	91.19% [0.67]	29.63%
ResNet-32	92.24%	-
MBS (L)	91.82% [0.42]	46.81%
ResNet-44	92.85%	-
MBS (L)	92.16% [0.69]	53.03%
ResNet-56	93.09%	-
MBS (L)	92.48% [0.61]	59.30%
ResNet-110	93.58%	-
MBS (L)	92.61% [0.97]	66.47%
ResNet-1202	94.04%	-
MBS (L)	93.06% [0.98]	72.71%
ResNet-110	93.58%	-
(Li et al. 2017) 110-A	93.55% [0.03]	2.30%
(Li et al. 2017) 110-B	93.30% [0.28]	32.40%
(Yu et al. 2018) NISP	93.35% [0.23]	43.25%
MBS ($3.4 \times L$)	93.47% [0.11]	50.29%

30 minutes on a PC with NVIDIA 1080-Ti for each pre-trained model on ImageNet. Notice that we only have to conduct first part once for each pre-trained model. The wall-clock time of second part is negligible, which is less than one second on the same PC.

Experiments

We applied MBS to various CNNs by PyTorch 0.3 on CIFAR-10 and ImageNet to evaluate its effectiveness in model reduction. Our experiments aim to answer three main questions:

1. How aggressively can one reduce the size of a CNN model without significantly degrading prediction accuracy?
2. Can MBS work effectively with deep and already highly compact CNN models?
3. Can MBS outperform competing model-reduction schemes?

Results on CIFAR-10 Dataset

CIFAR-10 consists of 50k training images and 10k testing images of 10 classes. We follow the training settings in (Huang et al. 2017): batch size is 128, weight decay is 10^{-4} , and learning rate is set to 0.1 initially and divided by 10 at the 50% and 75% of the total training epochs, respectively.

Accuracy and Reduction Tradeoff on ResNet We evaluated the effect of setting different receptive field size threshold z on prediction accuracy on CIFAR-10 with ResNet. The threshold z is set to $z = k \times L$, which k ranges from 1.4 to

Table 3: Model reduction results of CNN models with standard convolution on ImageNet.

Model	Top-1 [Diff.]	Top-5 [Diff.]	Parameters ($\times 10^6$)	Saving	Configuration
ResNet-18	69.76%	89.08%	11.69	-	[64, 128, 256, 512]
MBS (L)	69.40% [0.36]	88.88% [0.20]	9.94	14.97%	[64, 128, 256, 453]
ResNet-101	77.37%	93.56%	44.55	-	[64, 128, 256, 512]
MBS (L)	76.66% [0.72]	93.19% [0.37]	21.53	51.67%	[64, 128, 174, 337]
DenseNet-BC-121	74.65%	92.17%	7.98	-	$\beta = [1, 1, 1, 1]$
MBS (L)	74.35% [0.20]	91.92% [0.25]	6.04	24.31% $\beta = [1, 0.987, 0.832, 0.809]$	

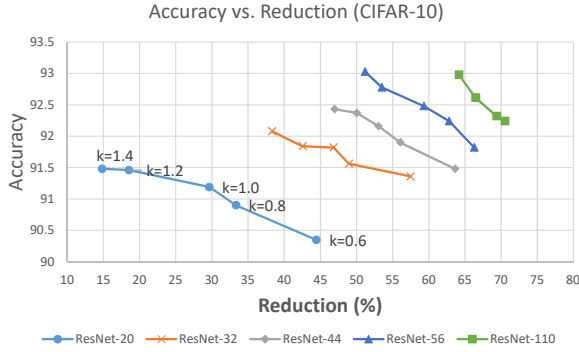


Figure 4: Tradeoff between accuracy and model reduction under different receptive field settings. The value k for $z = k \times L$ ranges from 1.4 to 0.6 with step 0.2 from the leftmost point to the rightmost point for each model.

0.6 with step size 0.2 from the leftmost point to the rightmost point for each model in Figure 4.

Figure 4 shows two results. The x -axis depicts model reduction ratio from low to high, and the y -axis prediction accuracy. We first observe that on all ResNet models (ResNet-20, 32, 44, 56, and 110), the more number of enhancement layers (i.e., MBS employing smaller z value, see the five z values on each line from large on the left to small on the right), the better the model reduction ratio. Second, the tradeoff between model reduction and prediction accuracy exhibits in all ResNet models, as expected.

The figure provides an application designer a perfect guidance to select the receptive field setting to fulfill the design goal. If accuracy out-weights model size, a larger k is desirable (i.e., fewer enhancement layers). If model size is the primary concern for power-conservation and frame-rate improvement (e.g., a video analysis requires 30fps), then the designer can select a small k . For instance, on ResNet-110, $k = 0.8$ achieves 70% model reduction with 1.26% loss in prediction accuracy.

MBS vs. Other Reduction Schemes Table 2 compares the reduction achieved by MBS and some representative methods. The top-half of the table lists our evaluation on all ResNet models. For instance, MBS reduces the model size of ResNet-1202 significantly (72.71%) with negligible accuracy drop (0.98%). The bottom half of the table compares

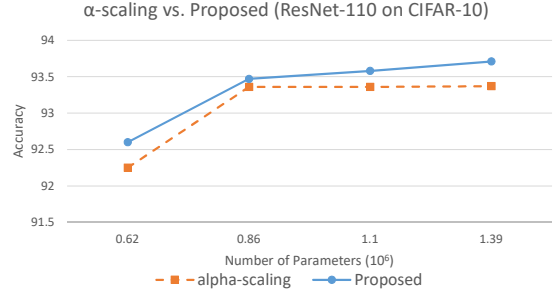


Figure 5: The x -axis denotes the model size and the y -axis represents the prediction accuracy. The α -scaling sets the α value ranges from 0.6 to 0.9 with step size 0.1. The proposed algorithm compares the performance with similar model size.

MBS with recently published methods with the best reduction ratios. We set MBS at the same accuracy level, MBS achieves the highest reduction ratio (50.29%).

We also compared MBS with the naive α -scaling method used by ResNet. The α -scaling multiplies the entire model with the same scaling factor α , whereas MBS adaptively sets the scaling factor by the information density of each macroblock. Figure 5 plots the range of α from 0.6 to 0.9 with step size 0.1. MBS outperforms α -scaling in prediction accuracy under four model sizes.

ImageNet Dataset

ImageNet has 1.28 million training images and 50k images for the 1,000 class validation. We trained all models (except for DenseNet, explained next) by 90 epochs with batch size set as 256. The learning rate is initially set to 0.1 and divided by 10 at epochs 30 and 60, respectively. For DenseNet, we trained its model by 100 epochs with batch size 128 and divided the learning rate by 10 at epochs 90 as suggested in (Huang et al. 2017). The data augmentation follows the ImageNet script of PyTorch, which is the same as ResNet (He et al. 2016). The weight decay is 10^{-4} for the CNNs with standard convolution (e.g., ResNet and DenseNet). The CNNs with depth-wise separable convolution (e.g., ShuffleNet and MobileNet) set the weight decay to 4×10^{-5} according to the training configurations as suggested in ShuffleNet (Zhang et al. 2017).

Table 4: Model reduction results of ResNet-34 on ImageNet.

	Top-1 [Diff.]	Top-5 [Diff.]	Parameters ($\times 10^6$)	Saving	Configuration
ResNet-34 (Original)	73.30%	91.42%	21.80	-	[64, 128, 256, 512]
(Li et al. 2017)	72.17% [1.13]	-	19.30	10.80%	-
(Yu et al. 2018) NISP-34-A	72.95% [0.35]	-	-	27.14%	-
(Yu et al. 2018) NISP-34-B	72.31% [0.99]	-	-	43.68%	-
MBS ($0.8 \times L$)	72.31% [0.99]	90.87% [0.55]	12.10	44.50%	[64, 128, 192, 359]

Table 5: Model reduction results of MobileNet and ShuffleNet on ImageNet.

Model	Top-1 [Diff.]	Top-5 [Diff.]	Parameters ($\times 10^6$)	Saving	Configuration
ShuffleNet ($g = 3$)	65.01%	85.89%	1.88	-	[24, 240, 480, 960]
Proposed (L)	63.95% [1.06]	85.15% [0.74]	1.49	20.74%	[24, 240, 444, 792]
MobileNet ($L = 224$)	70.73%	89.59%	4.23	-	[32, 64, 128, 256, 512, 1024]
Proposed (L)	70.52% [0.21]	89.57% [0.02]	4.00	5.43%	[32, 64, 128, 256, 512, 958]
Proposed ($0.8 \times L$)	69.90% [0.83]	89.21% [0.38]	3.50	17.26%	[32, 64, 128, 256, 474, 879]
MobileNet ($L = 192$)	68.88%	88.34%	4.23	-	[32, 64, 128, 256, 512, 1024]
Proposed (L)	68.98% [-0.10]	88.37% [-0.03]	3.93	7.10%	[32, 64, 128, 256, 512, 937]
Proposed ($0.8 \times L$)	68.05% [0.83]	87.77% [0.57]	3.14	25.77%	[32, 64, 128, 256, 441, 825]

Results of CNNs with Standard Convolution Table 3 shows that MBS is flexible to work with different CNN designs including very deep and complex CNN models such as ResNet-101 and DenseNet-121. As shown in Table 2, MBS can work with different depth configurations of ResNet on the CIFAR-10 dataset. Table 3 further shows consistent results when working on ImageNet. MBS achieves 51.67% model reduction for ResNet-101, while maintaining the same prediction accuracy. On a highly optimized deep model DenseNet-121 (a version of DenseNet-BC-121 defined in (Huang et al. 2017)), which has bottleneck modules and transition layers already highly compressed by 50%. MBS still can achieve additional 24.31% model reduction with negligible accuracy loss.

To exhaustively compare with all prior works, we also conducted experiments with ResNet-34. We divided the learning rate by 10 at epoch 90 and trained the reduced ResNet-34 with additional 10 epochs as a simplified fine-tune process. Table 4 shows that MBS is slightly better than state-of-the-art on ResNet-34 (by 0.8% at the same accuracy level).

Results of CNNs with Depth-wise Convolution We applied MBS to two CNN models with depth-wise convolution structures, ShuffleNet and MobileNet. The depth-wise convolution structure already reduces CNN model size significantly. Table 5 shows that MBS can further reduce these highly compact models. On ShuffleNet, MBS reduces the model size by additional 20.74% with negligible distortion. The depth-wise convolution and the unique shuffling operation of ShuffleNet would increase the difficulty of the objec-

tive function formulation for the optimization-based methods. On the contrary, MBS can simply estimate the channel-scaling factor for each CNN macroblock and perform model reduction.

We also evaluated MBS with MobileNet at different input image resolutions. Table 5 shows that MBS achieves 17.26% and 25.77% reduction on $L = 224$ and $L = 192$, respectively. Notice that when we set $z = L$, the prediction accuracy of MobileNet-192 improves slightly. This result suggests a possible smaller threshold value of z for MobileNet. Hence, we applied a slightly more aggressive setting of $z = 0.8 \times L$, which achieved a 25.77% model-size reduction.

Conclusion

We proposed a novel method to estimate the channel-scaling factor for each CNN macroblock. Our proposed MBS algorithm reduces model size guided by an information density surrogate without significantly degrading class-prediction accuracy. MBS is flexible in that it can work with various CNN models (e.g., ResNet, DenseNet, ShuffleNet and MobileNet), and is also scalable in its ability to work with ultra deep and highly compact CNN models (e.g., ResNet-1202). MBS outperforms all recently proposed methods to reduce model size at low computation complexity. With an adjustable receptive field parameter, an application designer can determine a proper tradeoff between prediction accuracy and model size (implying DRAM size and power consumption) by looking up a tradeoff table similar to the table presented in Figure 4.

References

- [Aghasi et al. 2017] Aghasi, A.; Abdi, A.; Nguyen, N.; and Romberg, J. 2017. Net-trim: Convex pruning of deep neural networks with performance guarantee. In *NIPS*. 3180–3189.
- [Courbariaux, Bengio, and David 2015] Courbariaux, M.; Bengio, Y.; and David, J.-P. 2015. Binaryconnect: Training deep neural networks with binary weights during propagations. In *NIPS*. 3123–3131.
- [Denton et al. 2014] Denton, E.; Zaremba, W.; Bruna, J.; LeCun, Y.; and Fergus, R. 2014. Exploiting linear structure within convolutional networks for efficient evaluation. In *NIPS*, NIPS’14, 1269–1277. Cambridge, MA, USA: MIT Press.
- [Figurnov et al. 2017] Figurnov, M.; Collins, M. D.; Zhu, Y.; Zhang, L.; Huang, J.; Vetrov, D.; and Salakhutdinov, R. 2017. Spatially adaptive computation time for residual networks. In *IEEE CVPR*.
- [Han et al. 2016] Han, S.; Liu, X.; Mao, H.; Pu, J.; Pedram, A.; Horowitz, M. A.; and Dally, W. J. 2016. Eie: Efficient inference engine on compressed deep neural network. *ISCA*.
- [Han, Mao, and Dally 2016] Han, S.; Mao, H.; and Dally, W. J. 2016. Deep compression: Compressing deep neural networks with pruning, trained quantization and Huffman coding. *ICLR*.
- [Hassibi and Stork 1993] Hassibi, B., and Stork, D. G. 1993. Second order derivatives for network pruning: Optimal brain surgeon. In *NIPS*, 164–171. San Francisco, CA, USA: Morgan Kaufmann Publishers Inc.
- [He et al. 2016] He, K.; Zhang, X.; Ren, S.; and Sun, J. 2016. Deep residual learning for image recognition. In *IEEE CVPR*.
- [He, Zhang, and Sun 2017] He, Y.; Zhang, X.; and Sun, J. 2017. Channel pruning for accelerating very deep neural networks. In *IEEE ICCV*.
- [Howard et al. 2017] Howard, A. G.; Zhu, M.; Chen, B.; Kalenichenko, D.; Wang, W.; Weyand, T.; Andreetto, M.; and Adam, H. 2017. Mobilenets: Efficient convolutional neural networks for mobile vision applications. *CoRR* abs/1704.04861.
- [Huang et al. 2017] Huang, G.; Liu, Z.; van der Maaten, L.; and Weinberger, K. Q. 2017. Densely connected convolutional networks. In *CVPR*.
- [Hubara et al. 2016] Hubara, I.; Courbariaux, M.; Soudry, D.; El-Yaniv, R.; and Bengio, Y. 2016. Binarized neural networks. In *NIPS*. 4107–4115.
- [Jaderberg, Vedaldi, and Zisserman 2014] Jaderberg, M.; Vedaldi, A.; and Zisserman, A. 2014. Speeding up convolutional neural networks with low rank expansions. In *BMVC*. BMVA Press.
- [Karmarkar 1984] Karmarkar, N. 1984. A new polynomial-time algorithm for linear programming. *Combinatorica* 4(4):373–395.
- [Krizhevsky, Sutskever, and Hinton 2012] Krizhevsky, A.; Sutskever, I.; and Hinton, G. E. 2012. Imagenet classification with deep convolutional neural networks. In *NIPS*, NIPS’12, 1097–1105.
- [Li et al. 2017] Li, H.; Kadav, A.; Durdanovic, I.; Samet, H.; and Graf, H. P. 2017. Pruning filters for efficient convnets. *ICLR*.
- [Lin, Zhao, and Pan 2017] Lin, X.; Zhao, C.; and Pan, W. 2017. Towards accurate binary convolutional neural network. In *NIPS*. 344–352.
- [Liu et al. 2015] Liu, B.; Wang, M.; Foroosh, H.; Tappen, M.; and Pensky, M. 2015. Sparse convolutional neural networks. In *IEEE CVPR*.
- [Liu et al. 2017] Liu, Z.; Li, J.; Shen, Z.; Huang, G.; Yan, S.; and Zhang, C. 2017. Learning efficient convolutional networks through network slimming. In *IEEE ICCV*.
- [Luo et al. 2016] Luo, W.; Li, Y.; Urtasun, R.; and Zemel, R. 2016. Understanding the effective receptive field in deep convolutional neural networks. In Lee, D. D.; Sugiyama, M.; Luxburg, U. V.; Guyon, I.; and Garnett, R., eds., *NIPS*. Curran Associates, Inc. 4898–4906.
- [Rastegari et al. 2016] Rastegari, M.; Ordonez, V.; Redmon, J.; and Farhadi, A. 2016. Xnor-net: Imagenet classification using binary convolutional neural networks. In *ECCV 2016*, 525–542.
- [Roffo, Melzi, and Cristani 2015] Roffo, G.; Melzi, S.; and Cristani, M. 2015. Infinite feature selection. In *IEEE ICCV 2015*, 4202–4210.
- [Simonyan and Zisserman 2014] Simonyan, K., and Zisserman, A. 2014. Very deep convolutional networks for large-scale image recognition. *CoRR* abs/1409.1556.
- [Sze et al. 2017] Sze, V.; Chen, Y. H.; Yang, T. J.; and Emer, J. S. 2017. Efficient processing of deep neural networks: A tutorial and survey. *Proceedings of the IEEE* 105(12):2295–2329.
- [Tang, Hua, and Wang 2017] Tang, W.; Hua, G.; and Wang, L. 2017. How to train a compact binary neural network with high accuracy? In *AAAI*.
- [Teerapittayanon, McDanel, and Kung 2016] Teerapittayanon, S.; McDanel, B.; and Kung, H. T. 2016. Branchynet: Fast inference via early exiting from deep neural networks. In editor., ed., *ICPR*.
- [Wen et al. 2016] Wen, W.; Wu, C.; Wang, Y.; Chen, Y.; and Li, H. 2016. Learning structured sparsity in deep neural networks. In *NIPS*. 2074–2082.
- [Wu et al. 2018] Wu, Z.; Nagarajan, T.; Kumar, A.; Rennie, S.; Davis, L. S.; Grauman, K.; and Feris, R. 2018. Block-drop: Dynamic inference paths in residual networks. In *IEEE CVPR*.
- [Yu et al. 2018] Yu, R.; Li, A.; Chen, C.-F.; Lai, J.-H.; Morariu, V. I.; Han, X.; Gao, M.; Lin, C.-Y.; and Davis, L. S. 2018. Nisp: Pruning networks using neuron importance score propagation. In *IEEE CVPR*.
- [Zhang et al. 2017] Zhang, X.; Zhou, X.; Lin, M.; and Sun, J. 2017. Shufflenet: An extremely efficient convolutional neural network for mobile devices. *CoRR* abs/1707.01083.